Knowles Partitioning at the Multi-reference Level

Ágnes Szabados,* András Gombás,* and Péter R. Surján*

Laboratory of Theoretical Chemistry, Institute of Chemistry, Faculty of Science, ELTE Eötvös Loránd University, H-1518 Budapest 112, P.O.B. 32, Hungary

E-mail: agnes.szabados@ttk.elte.hu; gombasandras@student.elte.hu; peter.surjan@ttk.elte.hu

Abstract

A multi-reference generalization of the partitioning introduced recently by Knowles (*J. Chem. Phys.* **2022** *156*, 011101) is presented with the aim to study electronic systems at a medium level of correlation. The multi-reference formalism applied is the general framework of multi-configuration perturbation theory (MCPT).

1 Introduction

Many-body methods[1,2] are ubiquitous in the description of electron correlation, following either perturbation theory (PT) or coupled-cluster (CC) considerations. Many-body PT (MBPT) has been established as a lower cost, lower performance option as compared to CC, applied in a variety of situations not only in molecular electronic structure[3–9] but also in vibrational structure[10,11] studies. Apart from being one of the pioneers of many-body methods, Professor Rodney Bartlett's leadership has been highly influential, shaping research in the field for a considerable period. It is not entirely without credit, that once, orienting a bewildered student in the enigmatic world of abbreviations in quantum chemistry, MBPT was jocularly resolved as "Mr. Bartlett's PT".

Considering the molecular electronic Hamiltonian, use of MBPT in its single-reference (SR) version mostly occurs in the Møller-Plesset (MP) partitioning,[12] where the Fockian is used as the zero-order Hamiltonian $\hat{H}^0$ and a single Hartree-Fock (HF) determinant constitutes the zero-order wave function. Applicability of this approach is limited to weakly correlated systems, where the exact full configuration interaction (FCI) wave function is dominated by the HF determinant.

Tuning low order MBPT corrections, e.g. with the intent of getting closer to truncated CC in terms of accuracy but not in terms of computational cost, has been an ever present challenge, even for weakly correlated systems. The theory in fact provides ground for this in leaving the partition of the Hamiltonian

$$\hat{H} \;=\; \hat{H}^0 \;+\; \hat{W} \tag{1}$$

up to choice. Among alternative options to MP,[13,14] Epstein-Nesbet partitioning is relatively well-known,[15–18] but many others were put forward (see e.g.[19,20] for review). Scaling an initial partitioning based on the idea of Feenberg[21,22] was extensively explored.[23–28] Thinking in terms of electron pairs has been fruitful in these considerations, revealing that the simplest variant of the coupled electron pair approximation (CEPA-0)[29] can be interpreted as a second-order PT method with non-MP partitioning. Zero-order Hamiltonians yielding CEPA-0 at second order were crafted based on matrix block-structure considerations,[30] restricting excitation implemented in a second-quantized expression of the operator,[31] as well as extending Feenberg's scaling to many parameters.[32,33] Of the surprisingly many alternative ways of recovering the CEPA-0 approximation,[34] infinite order resummation of MP terms[35–39] and linearized CC with double excitations (LCCD)[40] deserve mention here.

Setting up equations for parameters introduced in a zero-order Hamiltonian with the aim of improving some property of the arising PT terms is a strategy we are going to address as partitioning optimization. The method introduced by Knowles,[41] termed perturbation-

adapted PT (PAPT), is a partitioning optimization in line with previous efforts,[42–44] seeking an effective one-body potential suitable as zero-order operator for PT treatment. The PAPT equations, determining parameters (i.e. one-body integrals) in the second quantized expression of Knowles's H^0, can be interpreted as an internally-contracted variant of a multi-parameter extended Feenberg scaling.[45] Numerical assessment indicated that the ambition of getting PT2 energies closer to coupled-cluster singles and doubles (CCSD) is largely fulfilled by PAPT, admitting that scaling of the method also got similar to CCSD.[41,46]

Remarkable accuracy of PAPT in the SR framework gives the motivation of the present work. Regarding that Knowles's study is rooted in a SR formalism, results of numerical applications met expectations in finding its applicability limited to weak correlation.[46] The aim here is to extend the benefits of PAPT to situations where SRPT is inadequate, due to two or more determinants carrying considerable weight in the FCI wave function. Perturbative treatment in such situation calls for the application of a multi-reference (MR) version of the theory. Multi-reference extension of straightforward SR theories can be quite complicated.[47,48] The sheer number of MR-PT variants proposed in literature illustrates this statement, with a few selected examples given by[49–79] and references therein. From our present perspective, approaches that considered the idea of partitioning optimization in the MR setting are particularly interesting.[80–84] In view of the discussion above, MR realization of LCCD[85,86] and CEPA-0[87] are also related to partitioning optimization in spite of not utilizing PT terminology.

The MR framework chosen here for PAPT adaptation is a version termed multi-configuration perturbation theory (MCPT),[88] that already served for extension of the multi-parameter Feenberg's scaling.[84] Considerable numerical success of this effort was unfortunately matched with unfavorable computational cost (scaling with the third power of the dimension of the first-order interacting subspace of the Hilbert-space). System size dependence of the number of parameters to optimize in PAPT is a less steep function, giving the promise of a more practical approach. An MP-type partitioning variant of the MCPT framework[89] provides

an apt starting point that we shall review in the next Section. This is followed by a recap of Knowles's partitioning optimization in the SR context. Combination of these two building blocks is presented in Section 2.3. Numerical examples followed by a concluding Section closes the paper.

2 Theory

2.1 Review of MCPT

Given a normalized reference state which consists of a (usually limited) number of determinants

$$|\Phi\rangle \;=\; |0\rangle\, d_0 \;+\; \sum_{K=1}^{M} |K\rangle\, d_K, \tag{2}$$

where $|0\rangle$ is a principal determinant, aka pivot (e.g., Hartree-Fock, HF), while $|K\rangle$ denotes determinants excited from $|0\rangle$, a one-dimensional multi-reference projector is specified as

$$\hat{O} = |\Phi\;\rangle\langle\;\Phi|. \tag{3}$$

Determinants exhibiting a nonzero coefficient in the expansion of Φ span the reference space, which may be complete or incomplete. To set up a basis in the N-electron Hilbert space, we consider

1. the multi-configurational vector $|\Phi\rangle$;
2. excited determinants $|K\rangle$, constituting the reference space for $K = 1, \ldots, M$;
3. excited determinants $|K\rangle$, out of the reference space, i.e. $K = M + 1, \ldots$

Though the principal determinant has been dropped, the above specified basis is complete since $|0\rangle$ has nonzero coefficient in $|\Phi\rangle$.

Observe that $|\Phi\rangle$ and the excited determinants overlap. To account for this, we project

excited determinants by $\hat{P} = 1 - \hat{O}$ to get

$$|K'\rangle = \hat{P}|K\rangle = |K\rangle - |\Phi\rangle\, d_K, \tag{4}$$

projected determinants, which are orthogonal to $|\Phi\rangle$ but overlap among themselves. The overall metric matrix of the set $\{|\Phi\rangle\} \cup \{|K'\rangle | K = 1, \ldots, M\}$ exhibits the structure

$$\mathcal{S} = \begin{bmatrix} 1 & \mathbf{0} \\ \mathbf{0} & \mathbf{S} \end{bmatrix} \tag{5}$$

where elements of the diagonal block $\mathbf{S}$, assuming real coefficients read

$$S_{KL} = \langle K'|L'\rangle = \delta_{KL} - \langle K|\Phi\rangle\langle\Phi|L\rangle = \delta_{KL} \; - \; d_K \; d_L. \tag{6}$$

A key advantage of this metric is that it can be analytically inverted facilitating a biorthogonal perturbation theory,[90–94] where the bra basis vectors, transformed into the reciprocal space (denoted by tilde) have the following simple, two-determinantal expansion

$$\langle\widetilde{K'}| = \langle K| \; - \; \frac{d_K}{d_0}\, \langle 0|. \tag{7}$$

It can be seen by substitution, that $\langle\widetilde{K'}|L'\rangle = \delta_{KL}$ indeed holds.

In order to keep a closest possible resemblance with MP theory, we apply the zero-order of the MP-MCPT variant[89] in this work, which incorporates the generalized Fockian

$$F_{pq} = h_{pq} + \sum_{rs} \rho_{sr} [pr||qs] \tag{8}$$

in the zero-order Hamiltonian, with h_{pq} denoting one-electron integrals, $[pr||qs] = [pr|qs] - [pr|sq]$ standing for antisymmetrized two-electron integrals in Dirac-notation and ρ_{sr} being elements of the first-order density matrix constructed with the principal determinant. Small case latin

letters $p, q, \ldots$ are used for generic spinorbital indices. The zero-order Hamiltonian of MP-MCPT features a nondiagonal block in space $\hat{P}$, according to

$$\hat{H}^0_{\text{MP-MCPT}} \;=\; E^0\,\hat{O} \;+\; \hat{P}\,\hat{F}\,\hat{P}\;. \tag{9}$$

By construction, $|\Phi\rangle$ is an eigenvector of the zero-order operator with E^0 being the associated eigenvalue. Projected excited determinants $|K'\rangle$ are mixed by $\hat{H}^0_{\text{MP-MCPT}}$ as governed by the generalized Fockian.

The first-order equation for $|\Psi^1\rangle$ is written as

$$\big[\hat{H}^0 - E^0\big]|\Psi^1\rangle = -\hat{W}|\Phi\rangle \tag{10}$$

with $\hat{W} = \hat{H} - \hat{H}^0$. To solve Eq.(10), it is practical to introduce its coefficient matrix $\mathbf{T}$ with the elements

$$T_{LK} = \langle\widetilde{L'}|\hat{F} - E^0|K'\rangle\;, \quad K, L = 1, \ldots \tag{11}$$

Note, that the zero-order of Eq.(9) operates not only over the reference space but also over its orthogonal complement. In accordance with this, indices K and L above and further on run for *all* excited determinants. Notation $|K'\rangle$ and $\langle\widetilde{L'}|$ is somewhat superfluous for excited determinants out of the reference space, since Eqs.(4) and (7) obviously leave them intact. It is in the interest of brevity, that notation prime and tilde is kept for all excited determinants.

Expressing the first-order wavefunction as

$$|\Psi^1\rangle = \sum_{K=1} |K'\rangle c_K \tag{12}$$

first-order coefficients, obtained from the solution of Eq.(10) read

$$c_K = -\sum_{L=1} Q_{KL}\langle\widetilde{L'}|\hat{W}|\Phi\rangle \tag{13}$$

where Q_{KL} are elements of the reduced resolvent $\mathbf{Q}$, fulfilling

$$\mathbf{Q} = \mathbf{T}^{-1} \ . \tag{14}$$

With the help of Eqs.(12) and (13) the second-order energy is obtained as

$$E^2_{\text{MP-MCPT}} = \langle \Phi | \hat{W} | \Psi^1 \rangle = - \sum_{K=1} \langle \Phi | \hat{W} | K' \rangle \sum_{L=1} Q_{KL} \langle \widetilde{L'} | \hat{W} | \Phi \rangle \ . \tag{15}$$

Since we shall be dealing with the energy up to order three, the expression for the next order is given for completeness, assuming $\langle \Phi | \hat{W} | \Phi \rangle = 0$

$$E^3_{\text{MP-MCPT}} = - \sum_{K=1} \langle \Phi | \hat{W} | K' \rangle \sum_{L=1} Q_{KL} \langle \widetilde{L'} | \hat{W} | \Psi^1 \rangle \ . \tag{16}$$

Main characteristics of MP-MCPT in view of alternative schemes are briefly summarized below. For a more detailed account, see Ref.[89] The MCPT framework belongs to the diagonalize-then-perturb family of MR-PT methods. Regarding the choice of the zero-order Hamiltonian, MP-MCPT follows in the footsteps of Wolinsky and Pulay,[54] similarly to Roos's CAS based PT[56,73,74] or the formulation of Murphy and Messmer.[57] Use of a generalized Fockian for defining the zero-order is a characteristic shared by Hirao's multireference MP[59] also. Dyall's theory[63] and the n-electron valence state PT[67] introduced by Malrieu and coworkers are markedly different in including explicit two-body interaction at the level of the zero-order operator.

Basis vectors considered in the CI space is another, important aspect of MR-PT methodology, intimately tied to the question of overlap. By working on the basis of determinants in the first-order interacting subspace, MCPT represents a theory decontracted to the extreme. Were the overlap treated by means of a numerical algorithm,[54,56] a decontracted basis could seriously hinder practical use. Closed form of the inverse overlap, i.e. the expression of reciprocal functions by Eq.(7), is paramount in sidestepping numerical overlap handling.

To complete the picture, chief drawbacks of MP-MCPT, pivot dependence and size-inconsistency are to be mentioned. While the source of pivot-dependence is rather obvious, size-consistency violation is a more subtle issue. Size-inconsistency of MCPT, characterized previously by analytical as well as numerical means,[88,89] is a feature shared by MR-PT formulations that compose the zero-order Hamiltonian with the help of Hilbert-space projectors $\hat{O}$ and $\hat{P}$, c.f. Eq.(9).[64]

2.2 Review of the Knowles partitioning

In the framework of SR MBPT, in defining the zero-order Hamiltonian, Knowles[41] proposed to replace the Fockian with a nondiagonal one-body operator

$$\hat{\Lambda} \;=\; \sum_{ij} \Lambda_{ij} \quad i^+ j^- \;+\; \sum_{ab} \Lambda_{ab} \quad a^+ b^- \tag{17}$$

with elements Λ_{ij} and Λ_{ab} determined from the condition

$$\langle \Theta^+_{ij} | \, \hat{\Lambda}_N - \hat{H}_N \, | \Psi^1 \rangle = 0 \; , \tag{18a}$$

$$\langle \Theta^+_{ab} | \, \hat{\Lambda}_N - \hat{H}_N \, | \Psi^1 \rangle = 0 \; . \tag{18b}$$

In the above and throughout index convention $i, j, \ldots$ for occupied and $a, b, \ldots$ for virtual spinorbitals applies. Notation N in subscript refers to the normal ordered form of the operator, e.g. $\hat{H}_N = \hat{H} - \langle \mathrm{HF} | \hat{H} | \mathrm{HF} \rangle$. Many-body expression of the the first-order PT wave function is given by

$$\Psi^1 \;=\; \frac{1}{4} \sum_{ij} \sum_{ab} a^+ b^+ j^- i^- | \mathrm{HF} \rangle \; c^{ab}_{ij} \; , \tag{19}$$

with the first-order coefficients c^{ab}_{ij} being antisymmetric in indices ij and in indices ab. The projection manifold, $\langle \Theta^+_{ij}|$ and $\langle \Theta^+_{ab}|$ is a symmetrized version of an internal contraction of determinants constituting the first-order interacting subspace. In particular, for occupied

spinorbitals

$$\langle \Theta_{ij}| = \sum_{ab} \sum_{k} c_{ki}^{ab} \ \langle \mathrm{HF}|k^{+} j^{+} b^{-} a^{-}, \tag{20}$$

and

$$\langle \Theta_{ij}^{+}| = \langle \Theta_{ij}| + \langle \Theta_{ji}| \ , \quad i \leq j. \tag{21}$$

Analogous formulas apply for virtual projection functions. Assuming that Λ_{ij} and Λ_{ab} is symmetric, the number of projection equations matches the number of unknowns.

The significance of Eq.(18) is that the free parameters in the zero-order Hamiltonian $\hat{\Lambda}$ are determined from a condition that sets the effect of $\hat{\Lambda}$ as close as possible to that of $\hat{H}$ on the elements of the first-order interacting subspace (i.e. determinants interacting with $|\mathrm{HF}\rangle$ via the Hamiltonian). The second-order energy calculated as

$$E^{2}_{\text{SR-PAPT}} = \langle \mathrm{HF}|\hat{H}|\Psi^{1}_{\text{SR-PAPT}}\rangle \tag{22}$$

with $|\Psi^{1}_{\text{SR-PAPT}}\rangle$ obtained with $\hat{\Lambda}$ determined from Eq.(18), has been demonstrated to bring a considerable improvement over MBPT2.[41] Higher orders of the PT series have also improved as a consequence of parameters of the zero-order Hamiltonian fulfilling Eq.(18).

Note, that according to Eq.(17) no occupied-virtual mixing is allowed in Knowles' zero-order Hamiltonian. This means that the Brillouin theorem is preserved with all of its consequences in the SR version of Knowles' theory. This feature is going to abandoned in the MR version.

As demonstrated first numerically and later proved by formulae,[46] third-order correction by Knowles's partitioning vanishes when the procedure is iterated till self-consistency. First step of the iteration is obtained by constructing Eq.(20) with first-order coefficients in MP partitioning and generating first-order coefficients in Knowles's partitioning by the linear equations of Eq.(18). The latter coefficients substituted into Eq.(20) and the thus obtained projection functions applied in Eq.(18) yields a second iterate of $|\Psi^{1}\rangle$ in Knowles's partitioning. Assuming that convergence is attained by repeating this procedure, the third-order

energy can be given as

$$E^3_{\mathrm{SC}} = \langle \Psi^1_{\mathrm{SC}} | \hat{W}_N | \Psi^1_{\mathrm{SC}} \rangle \ , \tag{23}$$

where SC in subscript stands for self-consistence. Writing the first-order wavefunction in the form

$$\langle \Psi^1_{\mathrm{SC}} | = \frac{1}{2} \sum_i \langle \Theta^+_{ii} | \tag{24}$$

and taking into account that $\hat{W}_N$ is the negative of the operator appearing in Eq.(18), it is apparent that the Λ-conditions imposed by the diagonal functions, $\langle \Theta^+_{ii}|$ set individual terms of the third-order energy zero. (The argument can be equally written with Θ^+_{aa}.)

Completing the brief summary of PAPT, a note on the uniqueness of Λ-parameters is due. Though the number of equations in Eq.(18) formally matches the number of unknowns, it has been argued[41] that the number of independent equations is less by one. As observed in practice and demonstrated based on an SVD analysis of the coefficient matrix of the equations,[46] the normal ordered form, $\hat{\Lambda}_N$ appearing in Eq.(18) ensures that the undetermined linear combination of Λ-parameters corresponds to a shift of $\hat{\Lambda}$ by a constant, which is immaterial from the point of view of the subsequent PT treatment.

As long as the coefficient matrix of Eq.(18) features not more than one zero singular value, parameters in $\hat{\Lambda}$ are well defined. Appearance of two of more zero singular values would introduce an arbitrariness in the parameters. The SVD analysis of Ref.[46] indicates, that this might happen when a projection function or some linear combination of them were essentially orthogonal to the first order wavefunction and all single substitutions generated from it. Though in our practice we did not come across such a situation, it would be analogous to the instability of LCCD, and can be treated by standard techniques,[95,96] admitting that one of the many possible solutions is recovered this way.

2.3 Knowles partitioning in MCPT

Knowles' partitioning removes the arbitrariness regarding the value of the matrix-elements in the one-body zero-order Hamiltonian by requiring Eq.(18) in the SR context. In this section an analogous treatment is devised in the MR context. In MP-MCPT, matrix elements of the one-body operator entering the $\hat{P}$-block of Eq.(9) are allowed to become different from F_{pq} of Eq.(8).

Keeping notation $\hat{\Lambda}$ for the one-body operator including adjustable parameters, the zero-order Hamiltonian of PAPT- MCPT is written as

$$\hat{H}^0_{\text{PAPT-MCPT}} \;=\; \hat{P}\,\left(\hat{\Lambda} - \langle\hat{\Lambda}\rangle\right)\,\hat{P}\;, \tag{25}$$

where $\langle\hat{\Lambda}\rangle = \langle 0|\hat{\Lambda}|0\rangle$, with $|0\rangle$ being the principal determinant introduced in Eq.(2). Expression of $\hat{\Lambda}$ in the MR case reads

$$\hat{\Lambda} \;=\; \sum_{pq}\;\Lambda_{pq}\quad p^+q^-\;. \tag{26}$$

Note, that the index restriction of Eq.(17) is abandoned, which means stepping beyond the generalized MBPT[1,97] philosophy, where Λ_{ia} including terms would be assigned to perturbation.

The formalism of MCPT, operating with the concept of the principal determinant, is particularly suited for setting conditions for parameters Λ_{pq}. Though selection of a pivot introduces complications on its own, it provides a basis of occupied-virtual categorization that is inherent in the PAPT equations and can be applied in a straightforward manner. In addition, we posit the following features of the SR version of the theory to be conserved when formulating the MR extension

1. Λ-parameters should be unique, apart from a constant shift of $\hat{\Lambda}$;

2. $E^3_{\text{SC}} = 0$ should hold in the self-consistent case;

3. $\Lambda_{ia} = 0$ should hold in the limit where $|\Phi\rangle$ becomes single determinantal.

2.3.1 On requirement No. 1.

Item 1. above explains the structure of the P-block in Eq.(25). This term, entering the coefficient matrix of the PAPT equations, is decisive in the nature of the undetermined linear combination of Λ-parameters. According to an SVD analysis of the coefficient matrix of the equation,[46] a $\hat{\Lambda} - \langle\hat{\Lambda}\rangle$ type of expression is necessary in this term in order that the zero singular value is associated with a right singular vector of uniform coefficients. The latter describes a constant shift of $\hat{\Lambda}$, immaterial from the point of view of PT.

2.3.2 On requirement No. 2.

As a matter of convenience, the zero of the energy scale is fixed to $E^0 = \langle\Phi|\hat{H}|\Phi\rangle$, as reflected by the missing O-block in Eq.(25). In accordance with this

$$\hat{H}_N = \hat{H} \; - \; \langle\Phi|\hat{H}|\Phi\rangle \tag{27}$$

is applied, leading to $\langle\Phi|\hat{W}|\Phi\rangle = 0$, i.e. no first-order correction in the energy, since both terms of the perturbation operator

$$\hat{W} = \hat{H}_N - \hat{H}^0_{\text{PAPT-MCPT}} \tag{28}$$

exhibit zero expectation value with Φ.

We are now in a position to write the MR extension of the PAPT-equations, Eq.(18) as

$$\langle\Theta^+_{ij}|\, \hat{H}^0_{\text{PAPT-MCPT}} - \hat{H}_N\, |\Psi^1\rangle = 0 \;, \tag{29a}$$

$$\langle\Theta^+_{ab}|\, \hat{H}^0_{\text{PAPT-MCPT}} - \hat{H}_N\, |\Psi^1\rangle = 0 \;, \tag{29b}$$

with specification of the projection manifold being one of the remaining tasks. Theta func-

tions with two occupied or virtual indices are an extended version of Eq.(20), adapted to the MCPT framework. This means on one hand, that $\langle\Theta|$-s are expanded with reciprocal projected determinants, in line with the biorthogonal nature of the theory. On the other hand, single excitations are incorporated since they are elements of the first-order interacting subspace. Taking the case of two occupied indices, projection functions in the MCPT framework read

$$\langle\Theta_{ij}| = \frac{1}{2}\sum_{ab}\sum_{k}\widetilde{c}_{ki}^{ab}\ \widetilde{\langle 0_{ab}^{kj\,\prime}|}\ +\ \sum_{a}\widetilde{c}_{i}^{a}\ \widetilde{\langle 0_{a}^{j\,\prime}|}\ , \tag{30}$$

where $\widetilde{\langle 0_{ab}^{kj\,\prime}|}$ and $\widetilde{\langle 0_{a}^{j\,\prime}|}$ are reciprocal functions of projected, excited determinants $|0_{ab}^{kj\,\prime}\rangle = \hat{P}\,a^{+}b^{+}j^{-}k^{-}|0\rangle$ and $|0_{a}^{j\,\prime}\rangle = \hat{P}\,a^{+}j^{-}|0\rangle$ respectively, constructed with the help of Eq.(7). Symmetrization by Eq.(21) remains in effect. A formula analogous to Eq.(30) applies for $\langle\Theta_{ab}|$.

Coefficients $\widetilde{c}_{ki}^{ab}$ and $\widetilde{c}_{i}^{a}$ in Eq.(30) are chosen such that item 2. of the list of requirements is satisfied. For this end, the coefficient of $\widetilde{\langle L'|}$ in Eq.(16) is transcribed. Taking $|L\rangle = |0_{a}^{i}\rangle$ and applying the formula

$$\widetilde{c}_{i}^{a} = -\ \sum_{K=1}\langle\Phi|\hat{W}|K'\rangle Q_{KL} \tag{31}$$

gives the singly excited coefficient. The case of $\widetilde{c}_{ki}^{ab}$ is analogous, with $|L\rangle = |0_{ab}^{ki}\rangle$. Relation (14) between matrices $\mathbf{Q}$ and $\mathbf{T}$ persists. Elements T_{LK} are generated by the P-block of $\hat{H}^{0}_{\text{PAPT-MCPT}}$ as

$$T_{LK} = \widetilde{\langle L'|}\ \hat{\Lambda} - \langle\hat{\Lambda}\rangle\ |K'\rangle\ , \quad K,L = 1,\ldots \tag{32}$$

When constructing $\langle\Theta|$ functions for the first time, $\hat{\Lambda} = \hat{F}$ is used in Eq.(32), while the actual value of Λ-parameters is applied for obtaining $\Psi^{(1)}_{\text{PAPT-MCPT}}$ as well as for building $\langle\Theta|$ in course of a self-consistent iteration.

Comparing Eqs.(16) and (29), it is apparent that Eq.(29a) written with $\frac{1}{2}\langle\Theta_{ii}^{+}|$ obtained

from Eq.(30) gives terms of the third-order energy at the MR level. (An analogous statement is valid for Eq.(29b) and $\frac{1}{2}\langle\Theta^{+}_{aa}|.$)

2.3.3 On requirement No. 3.

Since Λ_{ia} parameters also appear in Eq.(26), further equations are necessary at the MR level, in addition to Eq.(29). These additional criteria are governed by item 3. of the list of requirements. Let us start by writing the first-order equation of the wavefunction, Eq.(10) partitioned for the space of single and double excitations as

$$\begin{pmatrix} T_{SS} & T_{SD} \\ T_{DS} & T_{DD} \end{pmatrix} \begin{pmatrix} \Psi^1_S \\ \Psi^1_D \end{pmatrix} = - \begin{pmatrix} (\hat{H}\Phi)_S \\ (\hat{H}\Phi)_D \end{pmatrix} . \tag{33}$$

Notation S and D in subscript refers to singly and doubly excited determinants, matrix elements and vector components written with the help of projected determinants in ket and their reciprocal counterparts in bra, in line with Eq.(32). The singles' block of the first-order wavefunction, Ψ^1_S is zero in the SR case, which rests on two things (i) $(\hat{H}\Phi)_S = 0$ due to the Brillouin-theorem and (ii) $T_{SD} = 0$ due to the lack of Λ_{ia} parameters. In the MR case neither of these holds, but we can set Λ_{ia} such that Ψ^1_S becomes zero. Inserting $\Psi^1_S = 0$ into Eq.(33) results

$$T_{SD}\Psi^1_D = -(\hat{H}\Phi)_S \tag{34}$$

$$T_{DD}\Psi^1_D = -(\hat{H}\Phi)_D \tag{35}$$

which can be combined into

$$T_{SD}T^{-1}_{DD}(\hat{H}\Phi)_D = (\hat{H}\Phi)_S\,. \tag{36}$$

Eq.(36) is essentially a first-order Brueckner condition,[98] providing as many equations as the number of Λ_{ia} parameters.

When applying Eq.(36) in the MR case, T_{DD}^{-1} is approximated by its diagonal form, leading to the following working form of the Λ-equations by singles projection for the PAPT-MCPT

$$\sum_{j}\sum_{b} R_{ia,jb}\ \Lambda_{jb} = \widetilde{\langle 0_a^{i\prime}|}\hat{H}_N|\Phi\rangle \tag{37}$$

with

$$R_{ia,jb} = \sum_{kl}\sum_{cd}\widetilde{\langle 0_a^{i\prime}|}j^+b^- + b^-j^+|0_{cd}^{kl\prime}\rangle\ \frac{\widetilde{\langle 0_{cd}^{kl\prime}|}\hat{H}_N|\Phi\rangle}{\widetilde{\langle 0_{cd}^{kl\prime}|}\hat{\Lambda} - \langle\hat{\Lambda}\rangle|0_{cd}^{kl\prime}\rangle}\ . \tag{38}$$

Note, that Eq.(37) is in fact nonlinear, Λ_{ii} and Λ_{aa} parameters entering the coefficient matrix of Eq.(38) via the denominator. In practice, the linearized form of Eq.(37) is solved in one step, together with Eq.(29). Elements $R_{ia,jb}$ are constructed with F_{ii} and F_{aa} substituted as Λ_{ii} and Λ_{aa} initially and the diagonal Λ-parameters are updated in course of a self-consistent PAPT iteration. Hence Λ_{ii} and Λ_{aa} become consistent in Eqs.(29) and (37) only upon convergence of a PAPT iteration. As a result of this and the approximative form of T_{DD}^{-1} in Eq.(38), the eventual contribution of single excitations to Ψ^1 of PAPT-MCPT is small, but nonzero.

2.3.4 Workflow of PAPT-MCPT

A flowchart in Fig. 1 gives an overview of the workflow of a PAPT-MCPT calculation. The first-order equation is initially solved with $\hat{F}$ applied in place of $\hat{\Lambda}$. This yields first-order wavefunction coefficients in MP partitioning and facilitates to compute projection functions, $\langle\Theta|$. Constructing quantities for the working equations of Λ-parameters, in particular Eq.(29) represents the rate determining step of the PAPT procedure. With Λ-parameters at hand, the first-order equation is solved again, to generate wavefunction coefficients in PAPT partitioning. The second-order energy in MP and PAPT partitionings is obtained from the

respective first-order wavefunction with the help of Eq.(15). In course of a self-consistent (SC) iteration, $\langle\Theta|$ functions are constructed again with the actual value of Λ-parameters fed into Eq.(32), and the process is repeated till convergence.

In the SR setting, rate determining step of the calculation is the construction of the coefficient matrix and inhomogeneous vector involved in Eq.(29), requiring manipulations scaling with the sixth power of the number of basis functions, with proper intermediates.[46] As indicated in Fig. 1, this remains essentially the same in the MR version. As long as the expansion in Eq.(12) resorts to single and double substitutions of the principal determinant, terms arising from non-pivotal components of the reference in Eq.(29) feature lower-order scaling. In this case, length of the expansion in Eq.(2) should contribute only to the overhead of the calculation cost. In the MR scenario, cost of the first-order wavefunction is to be considered too, as nondiagonal nature of matrix $\mathbf{T}$ makes it more costly than in the SR case. With a dense matrix $\mathbf{T}$, iterative solution of Eq.(10) would scale as $\sim n_{\mathrm{occ}}^4 \cdot n_{\mathrm{virt}}^4$, surpassing the cost of Eq.(29). However, the one-body nature of $\hat{F}$ or $\hat{\Lambda}$ renders matrix $\mathbf{T}$ comfortably sparse, allowing for the use of efficient, linear scaling algorithms, as it has been often stressed.[54]

3 Assessment

Test cases of the numerical assessment feature mild to serious challenge for the SR version of PAPT theory. Errors measured from FCI are shown in parallel for the MR and SR version of PT, the latter labeled PAPT-MBPT2 for Knowles' partitioning and MBPT2 for the original.

In our pilot applications special attention is paid since nonzero nature of Λ_{ia} parameters is an instance in what the MR generalization of PAPT markedly departs from the SR variant. The effect of single excitations can be easily switched off by resorting the expansion of the first-order wavefunction to double excitations. This is labeled by "-D" in the applications. To stress the inclusion of single excitations in addition to doubles, acronym "-SD" is used.

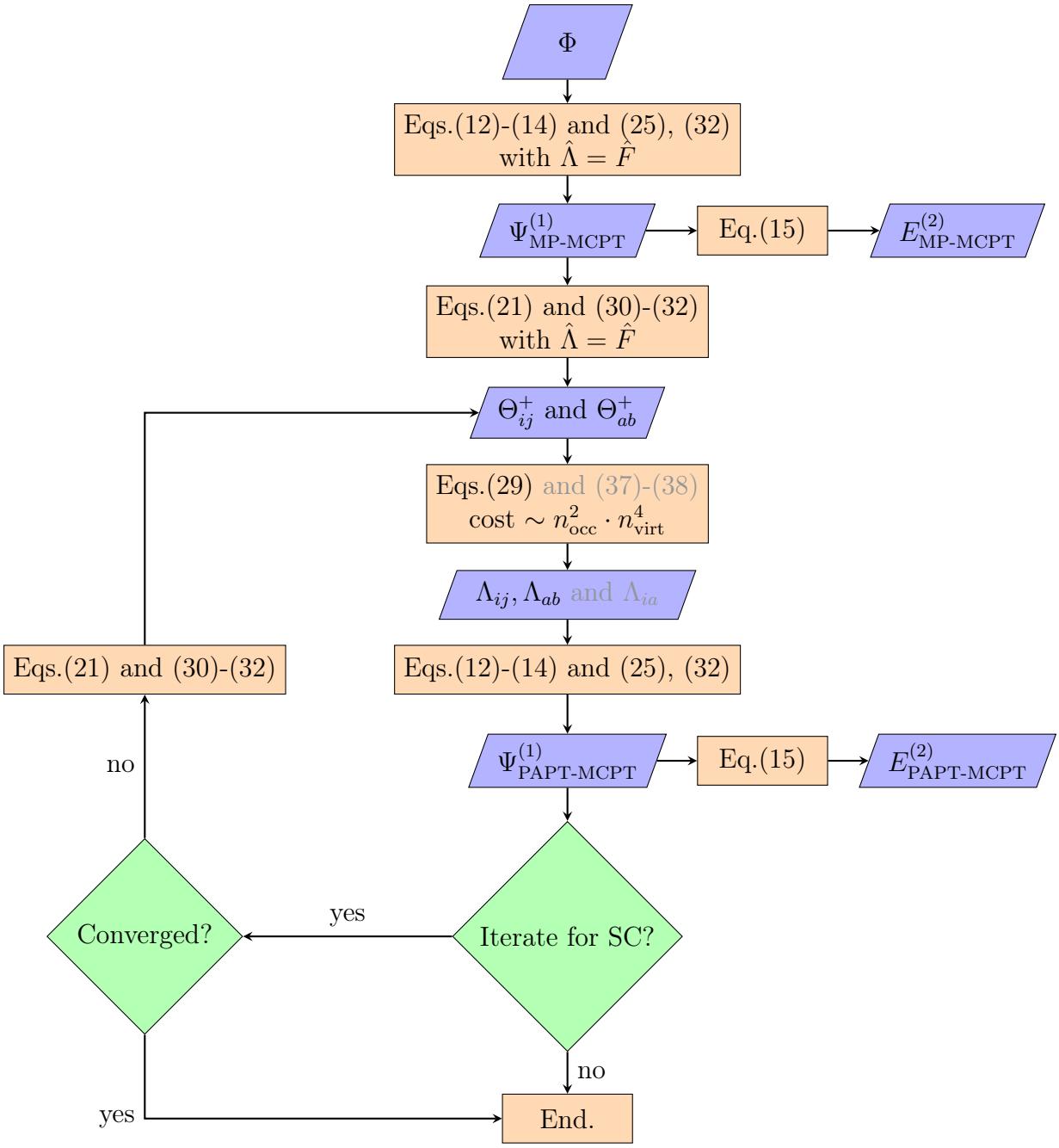

Figure 1: Flowchart of the PAPT-MCPT procedure. Gray font used for Eqs.(37)-(38) and Λ_{ia} indicates that these are not in effect in an exclusively doubles' procedure, c.f. Section 3.

The exclusively doubles' strategy removes the contribution of single excitations from projection functions, c.f. Eq.(30) and keeps $\Lambda_{ia} = 0$ in agreement with the fact that $(\hat{H}\Phi)_S$ is not constructed, c.f. Eqs.(36). In Fig. 1 Eqs.(37)-(38) and Λ_{ia} are typed with gray font to indicate that these are not in effect in an exclusively doubles' procedure.

Difficulties accompanying the MR generalization of PT are also demonstrated by a numerical characterization of size-inconsistency of the MP version of MCPT vis à vis its PAPT variant.

3.1 BeH_2 potential curve

The covalent bond cleavage and formation process is monitored with the help of the nine standardized geometry points (A-I) of Purvis and Bartlett.[99] The Be atom lays in the origin and the two H atoms are placed symmetrically to the z-axis with coordinates in atomic unit $(0, \pm 2.54, 0)$, $(0, \pm 2.08, 1.0)$, $(0, \pm 1.62, 2.0)$, $(0, \pm 1.39, 2.5)$, $(0, \pm 1.275, 2.75)$, $(0, \pm 1.16, 3.0)$, $(0, \pm 0.93, 3.5)$, $(0, \pm 0.70, 4.0)$, and $(0, \pm 0.70, 6.0)$, respectively. The process can be considered as the perpendicular insertion of a Be atom into a H_2 molecule, when advancing from point I to A.

The performance of PAPT-MCPT is monitored in cc-pVDZ basis set, taking either a two-determinantal CAS(2,2) or a perfect pairing generalized valence bond (GVB) function as reference. The latter corresponds to a direct product of two CAS(2,2) functions in the valence space, giving a total of four determinants contributing to Φ.

The CAS(2,2) active space is commonly constructed with the help of symmetry-conforming a_1 and b_2 molecular orbitals (MO) around the Fermi-level, taken e.g. from restricted HF (RHF). These two orbitals swap role along the process,[99] b_2 being more occupied at geometry points A-E and a_1 contributing more to the reference in the region F-I. Focusing on the mid region of the reaction path, active natural orbitals are displayed with occupation numbers in Fig.2. The two orbitals of fractional occupation numbers changing role between columns E ad F is apparent in the first row of Fig.2, labeled "CAS i.r. orbs.". In view that Purvis et al. reported on a symmetry-breaking RHF solution, it is not surprising that the CAS(2,2) wavefunction of proper symmetry corresponds to a local minimum on the parameters' hypersurface in the region A-F. A solution lower in energy by cca. 10-20 mE_h according to Table 1 can be constructed with orbitals not transforming according to any irreducible

representation (ir. rep., i.r.) of the molecular point group. These orbitals, depicted in the middle row of Fig.2 labeled "CAS non-i.r. orbs.", feature nearly equal population at the mid region. Unitary freedom is however given only with strict degeneracy of the populations (close to point F), leading to spatial symmetry breaking of the total wavefunction at all other arrangements in the A-F segment of the process. The "CAS non-i.r. orbs." orbitals at point E in Fig.2 largely resemble the symmetry-breaking set obtained by orbital-optimized pair-coupled cluster doubles,[100] with a reduced extent of quasi-degeneracy of occupation numbers. The spatial symmetry-breaking CAS(2,2) solution could not be continued beyond point F.

Active orbitals of the non-i.r. CAS(2,2) solution are also reminiscent of the natural orbitals of the GVB wavefunction at point E, where this model exhibits (near) degeneracy of the population of two MOs. An all valence GVB wavefunction for BeH_2 is composed of two (mutually orthogonal orbitals' built) CAS spaces, there are accordingly four orbitals with fractional occupation in the row labeled "GVB" in Fig.2. Character of the GVB natural MO's is again well known to be localized in space in regions where electron pairs reside mostly in accordance with chemical intuition. These orbitals vary the most along the reaction monitored: in region A-D they can be assigned to Be-H bonds (see column D in the last row of Fig.2), while in region F-I they can be assigned to the Be atom and the H_2 subunits of the system (c.f. column F). Geometry E represents a switching point for GVB, where natural MO's unusually delocalize, the wavefunction as well as its energy getting close to the global minimum CAS(2,2), c.f. Table 1. At other points of the reaction path, there is a further 8-20 mE_h energy gain when getting from the global minimum CAS(2,2) to GVB.

Figures 3-5 display second order MCPT results for these reference wavefunctions, proceeding in the order shown of Fig.2. Results by MBPT, based on the RHF determinant are included for comparison. In accordance with the increased multi-reference character of the system, errors shoot up in the mid region of the reaction pathway and are slightly larger in the G-H segment than at the starting, A-C interval. Performance of MCPT in reducing

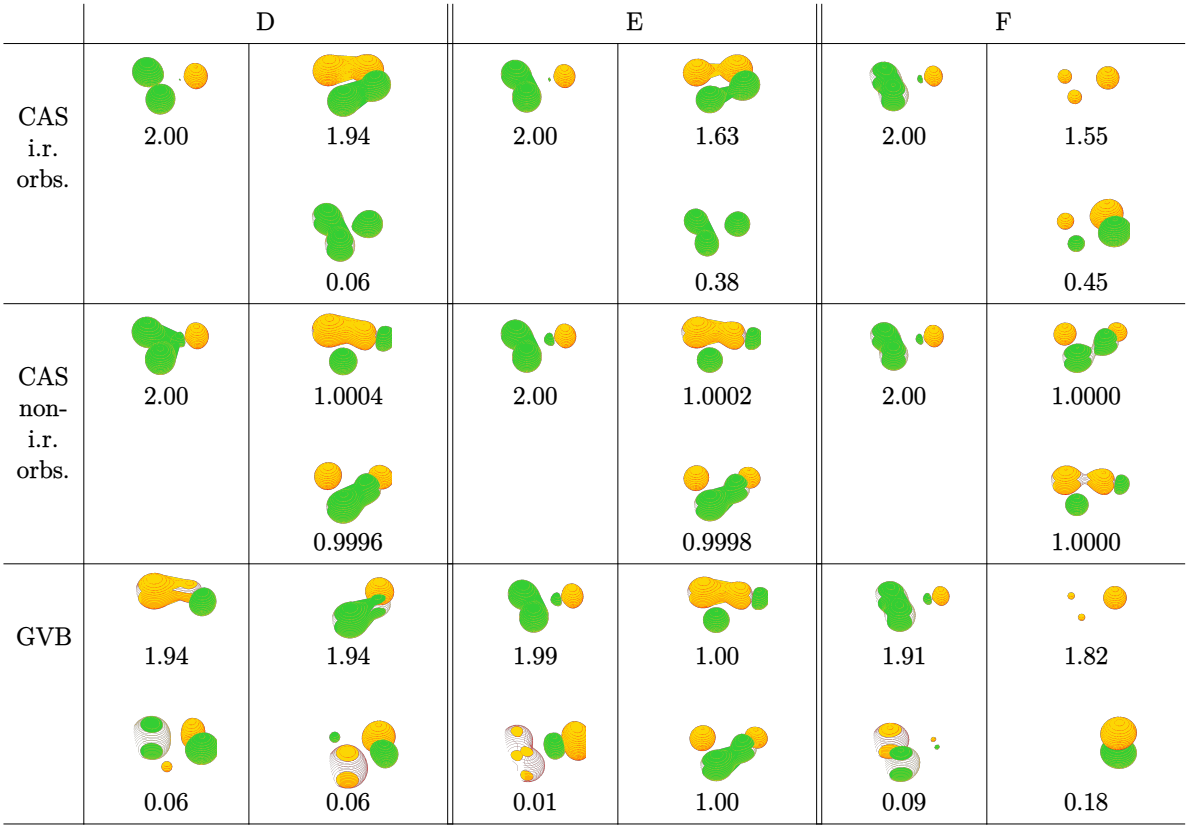

Figure 2: Natural orbitals of the valence shell for BeH_2 at geometry points D, E and F by CAS(2,2) and by valence GVB. Occupation numbers are given below the orbital contour plots. See text for more.

the error of MBPT improves with the increasing quality of the reference, in the order of Fig. 3, 4, 5. Point D in Fig. 4 is an exception, where MCPT errors are larger than those by MBPT. This is a consequence of the high open-shell character of the CAS(2,2) reference with non-ir. rep. orbitals, whereas either CAS(2,2) with ir. rep. orbitals or GVB provides a single, closed-shell determinant dominated picture. It is also immediately apparent in Figs. 3-5 that the numerical effect of the PAPT procedure is more significant than the step from single-reference to the multi-reference level. The former often improves the error by 80-99 %, while MCPT typically reduces the error of MBPT only by 5-50 %, omitting outliers both in the positive and negative direction.

To grab the effect of PAPT, thinner bar insets are to be compared with the surrounding

Table 1: Energy error of BeH_2 in mE_h by various reference functions in cc-pVDZ basis at standardized geometry points of Purvis and Bartlett.[99] For CAS(2,2), optimized orbitals are either irreducible representations of the molecular point group (i.r.) or not conforming with the molecular symmetry (non i.r.). See Fig. 2 for illustration.

geometry	$E - E_{FCI}$ (mE_h)		
	CAS(2,2)		GVB
	i.r. orbs.	non-i.r. orbs.	
A	67.8	56.2	45.0
B	65.6	57.7	45.5
C	72.5	57.4	40.4
D	77.8	56.0	39.7
E	98.2	55.2	55.2
F	75.8	55.5	47.5
G	69.5	n.a.[a)]	45.4
H	63.8	n.a.	46.4
I	62.5	n.a.	44.4

a): no solution with symmetry-breaking MO's could be located

thicker bars in the Figures. Focusing on PAPT at the MR level, the error of the original partitioning is uniformly and successfully reduced by PAPT. The magnitude of the effect however lags behind PAPT at the SR level, the latter mostly outperforming PAPT-MCPT2, apart from the highly challenging mid region. Regarding that PAPT-MCPT2 compares more favorably with PAPT-MBPT2 in the A-C interval, than in the G-I interval, this defect can be probably attributed to an imbalanced treatment of static and dynamic correlation in the MR level PAPT extension. In other words, PAPT-MCPT2 is more sensitive to the inadequacy of the pivot assumption than MP-MCPT2. This is also apparent from comparing parallelity of MP-MCPT2 and PAPT-MCPT2 along the reaction path, in any of the figures: the former curve is significantly more flat, than the latter. At the same time, the success of extending PAPT to the MR level is demonstrated by the results in E and F geometry points in Figs. 4, 5 and E in Fig. 3. In these cases PAPT-MBPT2 suffers seriously from the breakdown of the SR approximation, that is amended by an MR PAPT approach. Geometry point D remains challenging for PAPT-MCPT2, its shortcomings getting on the same footing with the defect of PAPT-MBPT2 in Figs. 3 and 5. The reason for PAPT-MCPT2 being considerably worse than PAPT-MBPT2 at point D in Fig. 4 is the highly open-shell character of the CAS(2,2)

wavefunction, vide supra.

Inclusion of single excitations has a negligible energetic effect both in the MP partitioning of MCPT and with PAPT-MCPT. This can be inferred from comparing error bars of "-D" methods with those of "-SD" in Figs. 3-5 and represents a justification of the strategy of treating single excitations in PAPT-MCPT2.

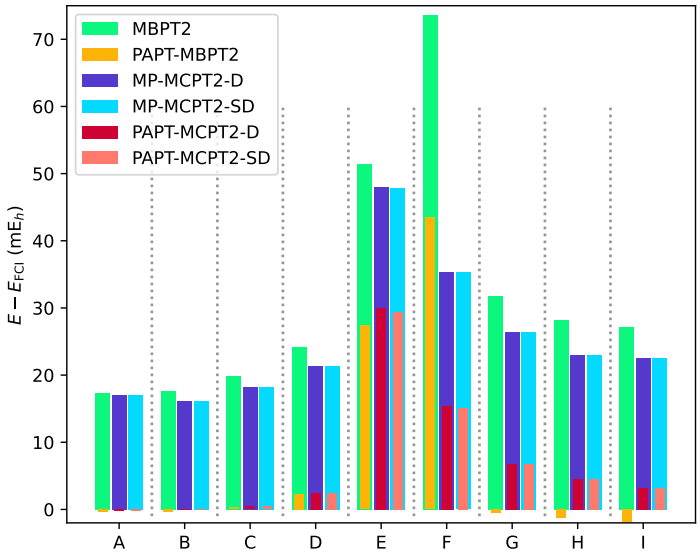

Figure 3: Energy error, $E - E_{\mathrm{FCI}}$ of BeH_2 in mE$_h$ by various partitionings in single-reference MBPT and multi-reference MCPT in cc-pVDZ basis at standardized geometry points of Purvis and Bartlett.[99] Reference function for MCPT is CAS(2,2), with ir. rep. optimized orbitals.

The result of solving the PAPT-equations in a self-consistent manner is displayed in Figs. 6-8. According to our numerical experience, self-consistent iteration of PAPT is highly sensitive to the treatment of single excitations. For this reason it was used as study case when crafting the singles' strategy according to Eq.(36). Our initial approach of formulating a singles' equation in the spirit of Eq.(29) was abandoned for notoriously destabilizing convergent SC-PAPT-MCPT iterations when stepping from exclusively doubles to a singles and doubles scheme. Thin bar insets in Figs. 6-8 indicate the result of self-consistent iteration with the surrounding thicker bars showing PAPT errors at the first iteration step. Wherever the thin inset is missing, convergence could not be reached with simple techniques, e.g. level-shift.

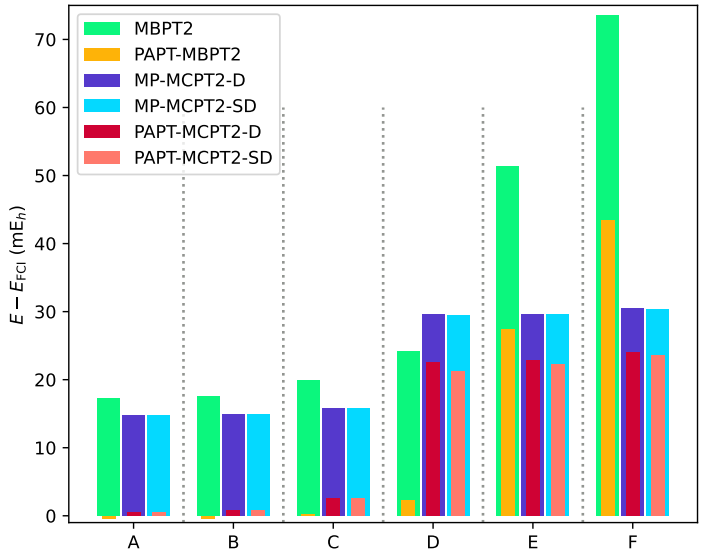

Figure 4: The same as Fig.3, with CAS(2,2) reference for MCPT, non-ir. rep. optimized orbitals.

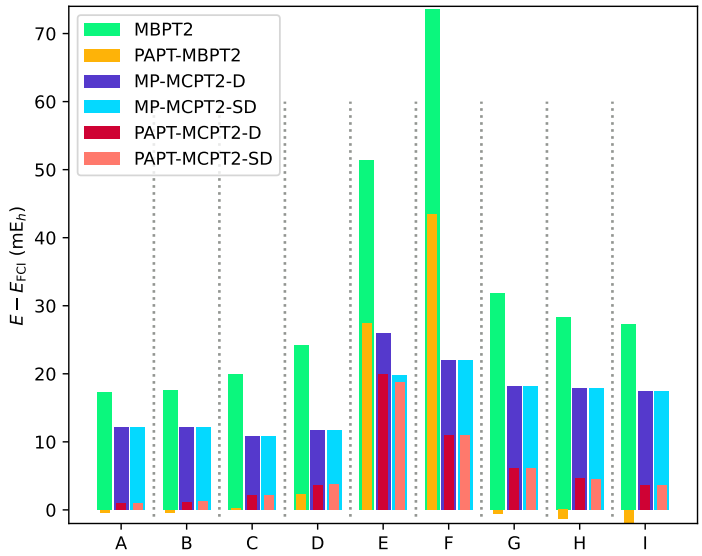

Figure 5: The same as Fig.3, with GVB reference for MCPT.

The marginal effect of singles in course of the self-consistent iteration can be grasped in Fig. 7: even the tiny energetic difference between the "-D" and "-SD" schemes is obliterated by SC. Altogether, Figs. 6-8 demonstrate that the effect of self-consistent iteration is rather negligible and does not seem worthy of the numerical effort, all the more so since

results occasionally deteriorate, c.f. points G-I with SC-PAPT-MBPT2 and point E with SC-PAPT-MCPT2 in Fig. 6.

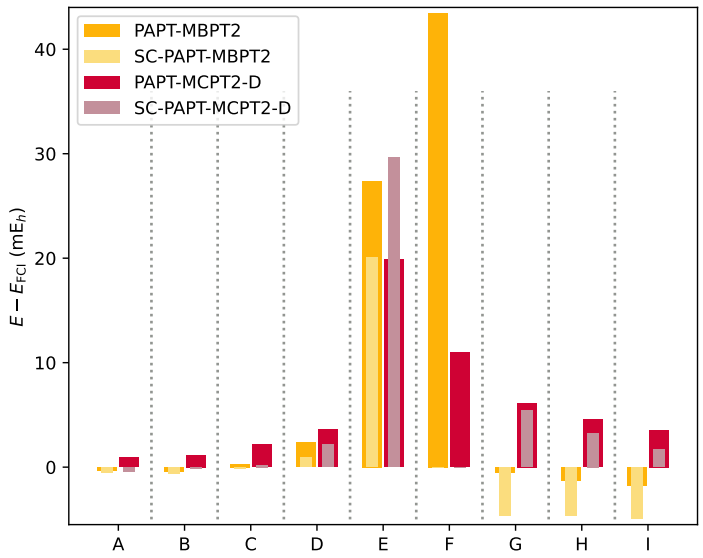

Figure 6: The same as Fig.3, with PAPT equations iterated till self-consistency.

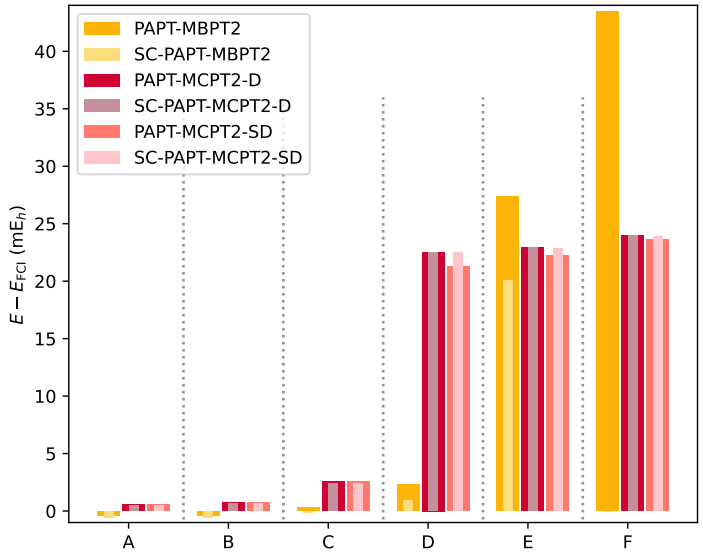

Figure 7: The same as Fig.4, with PAPT equations iterated till self-consistency.

HOMO-LUMO gaps collected in Table 2 provide an insight into the effect of partitioning optimization on the value of parameters. Inspecting the effect of PAPT equations of Eq.(29),

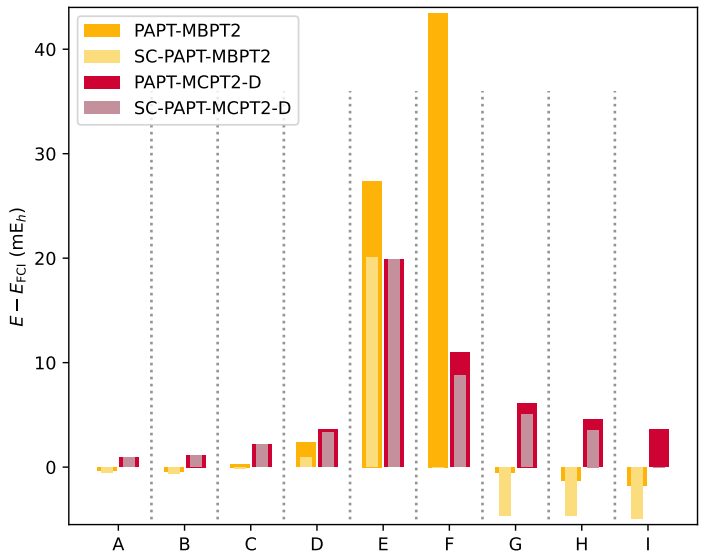

Figure 8: The same as Fig.5, with PAPT equations iterated till self-consistency.

the picture is similar in the SR and MR context. Comparing either MBPT2 with PAPT-MBPT2 or MP-MCPT2-SD with PAPT-MCPT2-D, we find that the gap of the one-body zero-order Hamiltonian closes for all cases shown in Table 2. When including Λ_{ia} parameters together with Eq.(37), the picture changes character: gaps in PAPT-MCPT2-SD rather open than close with respect to MP-MCPT2-SD. The only exception in Table 2 is the GVB reference at point F where the PAPT-MCPT2-SD gap is smaller than that of MP-MCPT2-SD, it is however larger than PAPT-MCPT2-D. The rather dramatic difference between PAPT-MCPT2-D and PAPT-MCPT2-SD gaps in Table 2 is in sharp contrast with the negligible energetic effect of single excitations in Figs. 3 and 5. The reason behind is that while Eq.(37) may generate rather large Λ_{ia} elements in absolute value in the off-diagonal block of $\mathbf{\Lambda}$, the Brueckner-condition suppresses their contribution to the first-order wavefunction.

Table 2: HOMO-LUMO gap in E_h of the one-body zero-order Hamiltonian, $\hat{F}$ or $\hat{\Lambda}$ in various PT schemes, for the BeH_2 system in cc-pVDZ basis. The Fockian is diagonalized for MBPT and MP-MCPT while eigenvalues of $\hat{\Lambda}$ are taken for PAPT-MBPT and PAPT-MCPT. Either a CAS(2,2) on i.r. optimized orbitals or GVB serves as reference.

	geometry D		geometry F	
MBPT2	0.2391		0.1748	
PAPT-MBPT2	0.1701		0.0572	
	CAS(2,2)	GVB	CAS(2,2)	GVB
MP-MCPT2-SD	0.2413	0.2466	0.2063	0.2088
PAPT-MCPT2-D	0.2204	0.1581	0.0053	0.0961
PAPT-MCPT2-SD	0.5234	0.3900	0.8813	0.1577

3.2 Size-inconsistency

Extensivity is a chief characteristic of many-body methods, often ensured via a diagrammatic formulation and relying on the linked cluster theorem.[1,2,40,101–103] With proper choice for the zero-order, extensivity of SR MBPT is thereby guaranteed. It has been shown in the SR case, that PAPT conserves extensivity of MBPT2.[41] However much extensivity is a desired property, PT methods at the MR level often violate it. In lack of connectivity arguments, it is customary to test the more easily attainable, closely related concept of size-consistency.

This Section presents numerical assessment of the effect of PAPT on size-inconsistency at the MR level. The test example is provided by two non-interacting LiH molecules in two basis sets. The results collected in Table 3 indicate that size-consistency violation is roughly doubled by the exclusively doubles' procedure, PAPT-MCPT2-D. Size-inconsistency is further accentuated by PAPT-MCPT2-SD in the 6-31G basis but remains unaffected in cc-pVDZ basis. This difference can be attributed to the appearance of Λ_{ia} parameters. In the 6-31G basis non-negligible core-virtual elements appear in $\mathbf{\Lambda}$. This increases size-inconsistency in line with previous observation on the role of off-diagonal blocks in the zero-order Hamiltonian matrix between different excitation levels in spoiling this property.[64] The cc-pVDZ basis remaining unaffected is explained by the fact that the core is frozen, and Λ_{ia} parameters with valence occupied indices remain insignificant. Altogether, inconsistency in the range of tenths of a mE_h to mE_h is to be compared to the second order correction to

the total energy falling in the order of 10 mE_h for the monomer.

Table 3: Size-consistency errors for the LiH dimer in mE_h. The reference state is a CAS(2,2) on the monomer, and their direct product for the dimer. Bond length of the monomer units is 2.00 Å . Core electrons are correlated in calculations in 6-31G basis and are frozen in cc-pVDZ basis.

basis set	6-31G	cc-pVDZ
MP-MCPT2-SD	0.12	0.54
PAPT-MCPT2-D	0.22	1.07
PAPT-MCPT2-SD	0.32	1.07

4 Conclusion

An extension of Knowles's recently introduced partitioning optimization to the MR level has been performed in the MP-MCPT framework. Pivot-dependence of the parent PT facilitates a relatively straightforward MR formulation, conserving main features of SR PAPT, in particular: i) vanishing third-order energy contribution in the self-consistent case; ii) uniqueness of the zero-order parameters apart from an immaterial constant shift and iii) compliance with the Brillouin-condition in the single-determinantal limiting case.

Numerical tests indicate that PAPT-MCPT2 successfully reduces the error of the original MP-type partitioning of MCPT. At the same time, apart from cases of significant MR character, performance of PAPT-MCPT2 falls behind that of PAPT at the SR level. This is attributed to an increased pivot dependence brought about by the MR level PAPT equations and motivates further efforts towards a pivot independent extension of the theory.

5 Acknowledgment

Part of the computations have been performed with the Budapest version of the MUNGAUSS program system.[104] Orbital contour plots have been prepared by the Molden package.[105] The FCI results were computed by an implementation of Olsen's FCI algorithm,[106] written in our lab by Zoltán Rolik (Budapest University of Technology and Economics).

References

(1) Shavitt, I.; Bartlett, R. J. *Many-Body Methods in Chemistry and Physics*; Cambridge University Press: Cambridge, 2009.

(2) Bartlett, R. J. Many-Body Perturbation Theory and Coupled Cluster Theory for Electron Correlation in Molecules. *Annual Review of Physical Chemistry* **1981**, *32*, 359–401.

(3) Sun, J.; Bartlett, R. Second-order many-body perturbation-theory calculations in extended systems. *J. Chem. Phys.* **1996**, *104*, 8553.

(4) Cremer, D. Møller–Plesset perturbation theory: from small molecule methods to methods for thousands of atoms. *Wiley Interdisciplinary Reviews: Computational Molecular Science* **2011**, *1*, 509–530.

(5) Grabowski, I.; Hirata, S.; Ivanov, S.; Bartlett, R. J. Ab initio density functional theory: OEP-MBPT(2). A new orbital-dependent correlation functional. *The Journal of Chemical Physics* **2002**, *116*, 4415–4425.

(6) Goerigk, L.; Grimme, S. Double-hybrid density functionals. *Wiley Interdiscip. Rev. Comput. Mol. Sci.* **2014**, *4*, 576–600.

(7) Phillips, J. J.; Zgid, D. Communication: The description of strong correlation within self-consistent Green's function second-order perturbation theory. *The Journal of Chemical Physics* **2014**, *140*, 241101.

(8) Hirata, S.; Doran, A. E.; Knowles, P. J.; Ortiz, J. V. One-particle many-body Green's function theory: Algebraic recursive definitions, linked-diagram theorem, irreducible-diagram theorem, and general-order algorithms. *The Journal of Chemical Physics* **2017**, *147*, 044108.

(9) Hirata, S. Finite-temperature many-body perturbation theory for electrons: Algebraic recursive definitions, second-quantized derivation, linked-diagram theorem, general-order algorithms, and grand canonical and canonical ensembles. *The Journal of Chemical Physics* **2021**, *155*, 094106.

(10) Christiansen, O. Møller–Plesset perturbation theory for vibrational wave functions. *The Journal of Chemical Physics* **2003**, *119*, 5773–5781.

(11) Barone, V.; Biczysko, M.; Bloino, J. Fully anharmonic IR and Raman spectra of medium-size molecular systems: accuracy and interpretation. *Phys. Chem. Chem. Phys.* **2014**, *16*, 1759–1787.

(12) Møller, C.; Plesset, M. Note on an approximation treatment for many-electron systems. *Phys. Rev.* **1934**, *46*, 618.

(13) Bartlett, R. J.; Silver, D. M. Many-body perturbation theory applied to electron pair correlation energies. I. Closed-shell first-row diatomic hydrides. *The Journal of Chemical Physics* **1975**, *62*, 3258–3268.

(14) Binkley, J. S.; Pople, J. A. Møller–Plesset theory for atomic ground state energies. *International Journal of Quantum Chemistry* **1975**, *9*, 229–236.

(15) Epstein, P. The stark effect from the point of view of Schroedinger's quantum theory. *Phys. Rev.* **1926**, *28*, 695.

(16) Nesbet, R. Configuration Interaction in Orbital Theories. *Proc. Roy. Soc. (London)* **1955**, *A230*, 312.

(17) Kvasnička, V. A second-quantization representation of the Epstein-Nesbet partitioning of the full hamiltonian. *Chemical Physics Letters* **1976**, *43*, 377 – 381.

(18) Malrieu, J.; Spiegelmann, F. Possible Artifacts Occurring in the Calculation of Inter-Molecular Energies from Delocalized Pictures. *Theor. Chim. Acta* **1979**, *52*, 55.

(19) Surján, P. R.; Szabados, Á. In *Fundamental World of Quantum Chemistry, A Tribute to the Memory of Per-Olov Löwdin*; Brändas, E. J., Kryachko, E. S., Eds.; Kluwer: Dordrecht, 2004; Vol. III; pp 129–185.

(20) Szabados, Á. *Reference Module in Chemistry, Molecular Sciences and Chemical Engineering*; Elsevier, 2017.

(21) Feenberg, E. Invariance Property of the Brillouin-Wigner Perturbation Series. *Phys. Rev.* **1956**, *103*, 1116.

(22) Goldhammer, P.; Feenberg, E. Refiriement of the Brillouin-Wigner Perturbation Method. *Phys. Rev.* **1955**, *101*, 1233.

(23) Forsberg, B.; He, Z.; He, Y.; Cremer, D. Convergence Behavior of the Møller-Plesset Perturbation Series: Use of Feenberg Scaling for the Exclusion of Backdoor Intruder States. *Int. J. Quantum Chem.* **2000**, *76*, 306–330.

(24) Bhattacharyya, K. Geometric Approximation in Rayleigh-Schrodinger Perturbation-Theory. *J. Phys. B* **1981**, *14*, 783.

(25) Schulman, J. M.; Musher, J. I. Hydrogen-atom Polarizability as a Hartree-Fock Perturbation Expansion - a Geometric Approximation to Atomic Polarizabilities. *J. Chem. Phys.* **1968**, *49*, 4845.

(26) Mukherjee, P. K.; Minato, T.; Chong, D. P. Finite-Field Calculations of Molecular Polarizabilities Using Field-Induced Polarization Functions. *Int. J. Quantum Chem.* **1983**, *23*, 447.

(27) Sadlej, A. J.; Wilson, S. Scaling, Pade Approximants and Variation Principles in the Many-Body Perturbation-Theory of Atomic and Molecular-Properties. *Mol. Phys.* **1981**, *44*, 299.

(28) Surján, P. R.; Szabados, Á. Size dependence of Feenberg scaling. *Int. J. Quantum Chem.* **2005**, *101*, 287–290.

(29) Ahlrichs, R.; Scharf, P. The Coupled Pair Approximation. *Adv. Chem. Phys.* **1987**, *67*, 501.

(30) Kutzelnigg, W. Note on the Perturbation Theory of Electron Correlation. *Chem. Phys. Letters* **1975**, *35*, 283.

(31) Fink, R. Two new unitary-invariant and size-consistent perturbation theoretical approaches to the electron correlation energy. *Chem. Phys. Letters* **2006**, *428*, 461.

(32) Szabados, Á.; Surján, P. R. Optimized partitioning in Rayleigh-Schrödinger perturbation theory. *Chem. Phys. Letters* **1999**, *308*, 303.

(33) Surján, P. R.; Szabados, Á. Optimized partitioning in perturbation theory: comparison to related approaches. *J. Chem. Phys.* **2000**, *112*, 4438–4446.

(34) Kutzelnigg, W. Density-cumulant functional theory. *The Journal of Chemical Physics* **2006**, *125*, 171101.

(35) Bartlett, R. J.; Shavitt, I. Comparison of High-Order Many-Body Perturbation Theory and Configuration Interaction for H2O. *Chem. Phys. Letters* **1977**, *50*, 190.

(36) Bartlett, R. J.; Shavitt, I. Comparison of High-Order Many-Body Perturbation Theory and Configuration Interaction for H2O. *Chem. Phys. Letters* **1978**, *57*, 157.

(37) Purvis, G. D.; Bartlett, R. J. Potential-Energy Curve for X1SIGMA-G+ State of Mg2 Calculated with Many-Body Perturbation-Theory. *J. Chem. Phys.* **1978**, *68*, 2114.

(38) Dietz, K.; Schmidt, C.; Warken, M.; Heß, B. A. On the acceleration of convergence of many-body perturbation theory. I. General theory. *J. Phys. B* **1993**, *26*, 1885.

(39) Dietz, K.; Schmidt, C.; Warken, M.; Heß, B. A. On the acceleration of convergence of many-body perturbation theory. II. Benchmark checks for small systems. *J. Phys. B* **1993**, *26*, 1897.

(40) Bartlett, R. J.; Purvis, G. D. Many-Body Perturbation-Theory, Coupled-Pair Many-Electron Theory, and Importance of Quadruple Excitations for Correlation Problem. *Int. J. Quantum Chem.* **1978**, *14*, 561.

(41) Knowles, P. J. Perturbation-adapted perturbation theory. *The Journal of Chemical Physics* **2022**, *156*, 011101.

(42) Kelly, H. P. Many-Body Perturbation Theory Applied to Atoms. *Phys. Rev.* **1964**, *136*, B896–B912.

(43) Silver, D. M.; Bartlett, R. J. Modified potentials in many-body perturbation theory. *Phys. Rev. A* **1976**, *13*, 1–12.

(44) Finley, J. P.; Freed, K. F. Application of complete space multireference many-body perturbation theory to N2: Dependence on reference space and H0. *J. Chem. Phys.* **1995**, *102*, 1306.

(45) Surján, P. R.; Kőhalmi, D.; Ágnes Szabados A Note on Perturbation-Adapted Perturbation Theory. *J. Chem. Phys.* **2022**, *156*, 116102.

(46) Gombás, A.; Surján, P. R.; Szabados, Á. Analysis and Assessment of Knowles' Partitioning in Many-Body Perturbation Theory. *Journal of Chemical Theory and Computation* **2024**, *20*, 5094–5104.

(47) Meissner, L. Multi-reference many-body perturbation theory and coupled cluster developments. *Molecular Physics* **2010**, *108*, 2961–2974.

(48) Bartlett, R. J. To Multireference or not to Multireference: That is the Question? *International Journal of Molecular Sciences* **2002**, *3*, 579–603.

(49) Hose, G.; Kaldor, U. Diagrammatic Many-Body Perturbation-Theory for General-model Spaces. *J. Phys. B* **1979**, *12*, 3827.

(50) Shavitt, I.; Redmon, L. T. Quasidegenerate perturbation theories. A canonical van Vleck formalism and its relationship to other approaches. *The Journal of Chemical Physics* **1980**, *73*, 5711–5717.

(51) Malrieu, J. P.; Durand, P.; Daudey, J. P. Intermediate Hamiltonians as a new class of effective Hamiltonians. *Journal of Physics A: Mathematical and General* **1985**, *18*, 809.

(52) Kucharski, S.; Bartlett, R. Multireference many-body perturbation theory. *Int. J. Quantum Chem.* **1988**, *S 22*, 383.

(53) Meissner, L.; Bartlett, R. J. The general model space effective Hamiltonian in order-for-order expansion. *J. Chem. Phys.* **1989**, *91*, 4800.

(54) Wolinski, K.; Pulay, P. Generalized Moller–Plesset perturbation theory: Second order results for two-configuration, open-shell excited singlet, and doublet wave functions. *J. Chem. Phys.* **1989**, *90*, 3647.

(55) Zarrabian, S.; Paldus, J. Applicability of multi-reference many-body perturbation theory to the determination of potential energy surfaces: A model study. *Int. J. Quantum Chem.* **1990**, *38*, 761.

(56) Andersson, K.; Malmqvist, P.-Å.; Roos, B. O.; Sadlej, A. J.; Wolinski, K. Second-order perturbation theory with a CASSCF reference function. *J. Phys. Chem.* **1990**, *94*, 5483.

(57) Murphy, R.; Messmer, R. Generalized Moller-Plesset Perturbation-Theory Applied to General MCSCF Reference Wave-Functions. *Chem. Phys. Letters* **1991**, *183*, 443.

(58) Duch, W.; Diercksen, G. Perturbation-Theory in Multireference Spaces. *Phys. Rev. A* **1992**, *46*, 95.

(59) Hirao, K. Multireference Moller-Plesset Method. *Chem. Phys. Letters* **1992**, *190*, 374.

(60) Nakano, H. Quasidegenerate perturbation theory with multiconfigurational self-consistent-field reference functions. *J. Chem. Phys.* **1993**, *99*, 7983.

(61) Cave, R. J.; Davidson, E. R. Hylleraas variational perturbation theory: Application to correlation problems in molecular systems. *J. Chem. Phys.* **1993**, *88*, 5770.

(62) Zaitsevskii, A.; Malrieu, J.-P. Multi-partitioning quasidegenerate perturbation theory. A new approach to multireference Møller-Plesset perturbation theory. *Chemical Physics Letters* **1995**, *233*, 597 – 604.

(63) Dyall, K. G. The choice of a zeroth-order Hamiltonian for second-order perturbation theory with a complete active space self-consistent-field reference function. *The Journal of Chemical Physics* **1995**, *102*, 4909–4918.

(64) van Dam, H. J. J.; van Lenthe, J. H.; Pulay, P. The size consistency of multi-reference Møller–Plesset perturbation theory. *Mol. Phys.* **1998**, *93*, 431.

(65) Mahapatra, U. S.; Datta, B.; Mukherjee, D. Molecular Applications of a Size-Consistent State-Specific Multireference Perturbation Theory with Relaxed Model-Space Coefficients. *The Journal of Physical Chemistry A* **1999**, *103*, 1822–1830.

(66) Davidson, E. R.; Jarzęcki, A. A. *Recent Advances in Multireference Methods*; World Scientific, 1999; Chapter 2, pp 31–63.

(67) Angeli, C.; Cimiraglia, R.; Evangelisti, S.; Leininger, T.; Malrieu, J.-P. Introduction of n-electron valence states for multireference perturbation theory. *The Journal of Chemical Physics* **2001**, *114*, 10252–10264.

(68) Chen, F.; Davidson, E.; Iwata, S. New time-independent perturbation theory for the multireference problem. *Int. J. Quantum Chem.* **2002**, *86*, 256.

(69) Shavitt, I. Multi-state Multireference Rayleigh–Schrödinger Perturbation Theory for Mixed Electronic States: Second and Third Order. *International Journal of Molecular Sciences* **2002**, *3*, 639.

(70) Khait, Y.; Song, J.; Hoffmann, M. Explication and revision of generalized Van Vleck perturbation theory for molecular electronic structure. *J. Chem. Phys.* **2002**, *117*, 4133–4145.

(71) Rosta, E.; Surján, P. R. Two-body zeroth order Hamiltonians in multireference perturbation theory: The APSG reference state. *J. Chem. Phys.* **2002**, *116*, 878.

(72) Evangelista, F. A.; Simmonett, A. C.; Schaefer III, H. F.; Mukherjee, D.; Allen, W. D. A companion perturbation theory for state-specific multireference coupled cluster methods. *Phys. Chem. Chem. Phys.* **2009**, *11*, 4728–4741.

(73) Pulay, P. A perspective on the CASPT2 method. *International Journal of Quantum Chemistry* **2011**, *111*, 3273–3279.

(74) Roca-Sanjuán, D.; Aquilante, F.; Lindh, R. Multiconfiguration second-order perturbation theory approach to strong electron correlation in chemistry and photochemistry. *WIREs Computational Molecular Science* **2012**, *2*, 585–603.

(75) Chen, Z.; Hoffmann, M. R. Orbitally invariant internally contracted multireference unitary coupled cluster theory and its perturbative approximation: Theory and test calculations of second order approximation. *The Journal of Chemical Physics* **2012**, *137*, 014108.

(76) Rolik, Z.; Kállay, M. A second-order multi-reference quasiparticle-based perturbation theory. *Theoretical Chemistry Accounts* **2015**, *134*, 143.

(77) Chattopadhyay, S.; Chaudhuri, R. K.; Mahapatra, U. S.; Ghosh, A.; Ray, S. S. State-specific multireference perturbation theory: development and present status. *WIREs Computational Molecular Science* **2016**, *6*, 266–291.

(78) Lang, L.; Sivalingam, K.; Neese, F. The combination of multipartitioning of the Hamiltonian with canonical Van Vleck perturbation theory leads to a Hermitian variant of quasidegenerate N-electron valence perturbation theory. *The Journal of Chemical Physics* **2020**, *152*, 014109.

(79) Kollmar, C.; Sivalingam, K.; Neese, F. An alternative choice of the zeroth-order Hamiltonian in CASPT2 theory. *The Journal of Chemical Physics* **2020**, *152*, 214110.

(80) Finley, J. P.; Chaudhuri, R. K.; Freed, K. F. Applications of multireference perturbation theory to potential energy surfaces by optimal partitioning of H: Intruder states avoidance and convergence enhancement. *J. Chem. Phys.* **1995**, *103*, 4990.

(81) Chaudhuri, R. K.; Finley, J. P.; Freed, K. F. Comparison of the perturbative convergence with multireference Möller–Plesset, Epstein–Nesbet, forced degenerate and optimized zeroth order partitionings: The excited BeH2 surface. *J. Chem. Phys.* **2001**, *106*, 4067.

(82) Witek, H. A.; Nakano, H.; Hirao, K. Multireference perturbation theory with optimized partitioning. I. Theoretical and computational aspects. *J. Chem. Phys.* **2003**, *118*, 8197–8206.

(83) Witek, H. A.; Nakano, H.; Hirao, K. Multireference perturbation theory with optimized partitioning. II. Applications to molecular systems. *J. Comput. Chem.* **2003**, *24*, 1390–1400.

(84) Surján, P. R.; Rolik, Z.; Szabados, Á.; Kőhalmi, D. Partitioning in multiconfiguration perturbation theory. *Ann. Phys. (Leipzig)* **2004**, *13*, 223–231.

(85) Laidig, W. D.; Saxe, P.; Bartlett, R. J. The description of N2 and F2 potential energy surfaces using multireference coupled cluster theory. *J. Chem. Phys.* **1987**, *86*, 887.

(86) Zoboki, T.; Szabados, Á.; Surján, P. R. Linearized Coupled Cluster Corrections to Antisymmetrized Product of Strongly Orthogonal Geminals: Role of Dispersive Interactions. *J. Chem. Theory Comput.* **2013**, *9*, 2602–2608.

(87) Szalay, P. G. Towards State-Specific Formulation of Multireference Coupled-Cluster Theory: Coupled Electron Pair Approximations (CEPA) Leading to Multireference Configuration Interaction (MR-CI) Type Equations. *Recent Advances in Computational Chemistry* **1997**, *3*, 81–123.

(88) Rolik, Z.; Szabados, Á.; Surján, P. R. On the perturbation of multiconfiguration wave functions. *J. Chem. Phys.* **2003**, *119*, 1922.

(89) Kobayashi, M.; Szabados, Á.; Nakai, H.; Surján, P. R. Generalized Møller-Plesset Partitioning in Multiconfiguration Perturbation Theory. *J. Chem. Theory Comput.* **2010**, *6*, 2024–2033.

(90) Gouyet, J. F. Use of biorthogonal orbitals in calculation by perturbation of molecular interactions. *J. Chem. Phys.* **1973**, *59*, 4637.

(91) Gouyet, J. F. Use of biorthogonal orbitals in perturbation calculation of molecular interactions from a multiconfigurational unperturbed state. *J. Chem. Phys.* **1974**, *60*, 3690.

(92) Surján, P. R.; Mayer, I.; Lukovits, I. Interaction of chemical bonds. II. Ab initio theory for overlap, delocalization, and dispersion interactions. *Phys. Rev. A* **1985**, *32*, 748.

(93) Surján, P. R.; Mayer, I.; Lukovits, I. Second-quantization-based perturbation theory for intermolecular interactions without basis set superposition error. *Chem. Phys. Letters* **1985**, *119*, 538.

(94) Surján, P. R.; Mayer, I. Intermolecular Interactions - Biorthogonal Perturbation-Theory Revisited. *J. Mol. Struct.* (THEOCHEM) **1991**, *226*, 47.

(95) Israel, A. B.; Greville, T. *Generalized Inverses: Theory and Applications, (2nd ed.)*; Springer,: New York, 2003.

(96) Taube, A. G.; Bartlett, R. J. Rethinking linearized coupled-cluster theory. *J. Chem. Phys.* **2009**, *130*, 144112.

(97) Bartlett, R. J. In *Coupled-cluster theory: an overview of recent developments, in: Modern electronic Structure Theory, part I.*; Yarkony, D. R., Ed.; World Scientific: Singapore, 1995; p 1047.

(98) Nesbet, R. Brueckner's Theory and the Method of Superposition of Configurations. *Phys. Rev.* **1958**, *109*, 1632.

(99) Purvis, G.; Shepard, R.; Brown, F.; Bartlett, R. C2V Insertion pathway for BeH2: A test problem for the coupled-cluster single and double excitation model. *Int. J. Quantum Chem.* **1983**, *23*, 835–845.

(100) Boguslawski, K.; Tecmer, P.; Bultinck, P.; De Baerdemacker, S.; Van Neck, D.; Ayers, P. W. Nonvariational Orbital Optimization Techniques for the AP1roG Wave Function. *Journal of Chemical Theory and Computation* **2014**, *10*, 4873–4882.

(101) Nooijen, M.; Shamasundar, K.; Mukherjee, D. Reflections on size-extensivity, size-consistency and generalized extensivity in many-body theory. *Mol. Phys.* **2005**, *103*, 2277–2298.

(102) Lyakh, D. I. Algebraic connectivity analysis in molecular electronic structure theory I: coulomb potential, tensor connectivity, ϵ-approximation. *Molecular Physics* **2012**, *110*, 1469–1492.

(103) Lyakh, D. I.; Bartlett, R. J. Algebraic connectivity analysis in molecular electronic structure theory II: total exponential formulation of second-quantised correlated methods. *Molecular Physics* **2014**, *112*, 213–260.

(104) Poirier, R. A.; Peterson, M. MUNGAUSS program suite. *Dept. Chemistry, Memorial Univ.St.Johns* **1989**

(105) Schaftenaar, G.; Noordik, J. H. Molden: a pre- and post-processing program for molecular and electronic structures. *J. Comput.-Aided Mol. Design* **2000**, *14*, 123–134.

(106) Olsen, J.; Roos B. O., Jørgensen, P.; Jensen, H. J. A. Determinant based configuration interaction algorithms for complete and restricted configuration interaction spaces *J. Chem. Phys.* **1988**, *89*, 2185–2192.

TOC Graphic